AQUA
Water Infrastructure, Ecosystems and Society

IWA PUBLISHING

 AQUA — Water Infrastructure, Ecosystems and Society Vol 72 No 10, 1825 doi: 10.2166/aqua.2023.014

Using image texture to monitor the growth and settling of flocs

Qidong Ma [a,b], Yan Liu[a], Zhangwei He[a,b], Haiguang Wang[a,b], Ruolan Wang[a,b], Yueping Kong[b,c] and Zhihua Li [a,b,*]

[a] Key Laboratory of Northwest Water Resource, Environment, and Ecology, MOE, School of Environmental and Municipal Engineering, Xi'an University of Architecture and Technology, Xi'an 710055, China
[b] Xi'an Key Laboratory of Intelligent Equipment Technology for Environmental Engineering, Xi'an University of Architecture and Technology, Xi'an 710055, China
[c] School of Information and Control Engineering, Xi'an University of Architecture and Technology, Xi'an 710055, China
*Corresponding author. E-mail: lizhihua@xauat.edu.cn

QM, 0000-0003-1023-8533; ZL, 0000-0002-4643-6331

ABSTRACT

Currently, a reliable and easy-to-use method to monitor flocculation in the water treatment process is highly demanded, especially for small water purification stations. For this problem, *in situ* images were used to analyze the flocculation process under different conditions via jar tests. A texture feature of the gray level co-occurrence matrix was found to be helpful for monitoring the floc status, such as growth rate and settling velocity. To further verify this finding, we established the correlation between the texture time sequence curve (TTSC) and its corresponding floc status. The slope of the TTSC during the growth phase and during the settling phase can describe the growth rate and the settling velocity, respectively, i.e., the higher the slope, the higher the growth rate and settling velocity. In addition, significant differences between the TTSCs in various abnormal conditions and the normal condition of coagulation can be identified. By using the TTSC for detecting abnormal conditions, we again verified that the texture feature can reliably reflect the flocculation process. Our study helps to develop a low-cost, stable, and simple method for monitoring flocculation and detecting abnormal conditions, which can effectively be used in the operation and management of water treatment plants.

Key words: abnormal conditions, flocculation, floc image, texture features

HIGHLIGHTS

- Compared with the morphological features, the texture features are more stable.
- The texture time sequence curve (TTSC) can describe flocculation.
- Variation characteristics of TTSC can detect abnormal coagulation conditions.
- TTSC-based methods can be readily applied online.

GRAPHICAL ABSTRACT

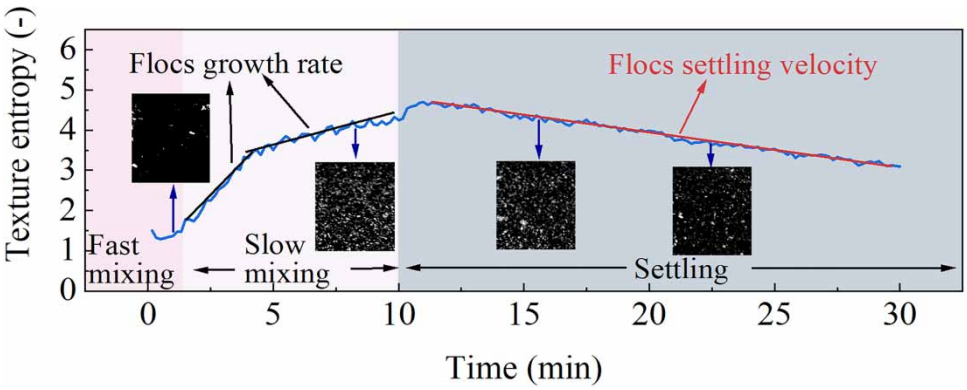

1. INTRODUCTION

Coagulation and sedimentation are both well-known and essential purification processes in water treatment. Coagulation is a process that makes colloidal particles, which destabilizes and then aggregates into flocs (Ekeleme *et al.* 2021; Ismail *et al.* 2022). The effluent quality of the purification process is largely determined by the coagulation effect (Matilainen *et al.* 2010). Sedimentation is a process in which the formed flocs are settled and removed by gravity. If the flocs are not settled completely, an increase in the turbidity of the effluent will result (Peña-Guzmán & Ortiz-Gutierrez 2022). In these mentioned processes, the growth rate and settling velocity are two crucial indicators for monitoring floc status (Adachi & Tanaka 1997; Bo *et al.* 2012). Thus, it is essential to accurately monitor the above two indicators for water supply safety and the operation optimization of water treatment plants (WTP).

Nowadays, there are three major tools to monitor the growth rate of flocs: laser particle size analyzer, photometric dispersion analyzer (PDA), and computational vision. The laser particle size analyzer is an instrument that measures particle size and distribution based on the light scattering principle, and it is widely used in the study of floc growth and morphology (Liu *et al.* 2021). PDA is an instrument to monitor floc strength and growth rate with the technique of transmitted light fluctuation (Wu *et al.* 2012). However, these two instruments are mostly applicable in the laboratory. Their feasibility is challenged in field studies and WTP online monitoring due to complications, fragility, and high maintenance.

Popular methods for measuring settling velocity include the floc settling model, particle image velocimetry (PIV), and computational vision. The floc settling model is a prediction model based on Stokes' law, which could determine the settling velocity with floc size, fractal dimension, water density, viscosity, and other parameters (Vahedi & Gorczyca 2012). However, this model is limited to theoretical study, and it is difficult to apply in practice because it involves too many variables and is still under modification and development. PIV is a measuring instrument of settling velocity based on image analysis technology (Xiao *et al.* 2011), which is also difficult to apply in the WTP due to complex operation and high cost.

In brief, a reliable and easy-to-use method to monitor flocculation in the WTP is in high demand. In recent years, computational vision has been increasingly applied to monitor the shape and status of floc. Especially thanks to the cost reduction of the industrial camera and the development of image processing algorithms, it is possible to apply computational vision to the WTP (Tomperi *et al.* 2016). For example, some researchers analyzed the relationship between sludge color and operating conditions and then devised a method for monitoring sludge status and hydraulic conditions using color space (Li *et al.* 2019). There are also studies evaluating the strength of Al-humus and Al-kaolin flocs according to the *in situ* images (Moruzzi *et al.* 2019), exploring a new way to monitor floc strength using computational vision. As mentioned above, computational vision is also applied to measure and monitor the growth rate and settling velocity of flocs. Nevertheless, when flocs are abundant in the water, the flocs are easy to be lost, overlapped, and out of focus, so the data error will be too serious, leading to unreliable results. This method requires analyzing the characteristics of a single floc in the image, which is challenging when the concentration of floc particles is high. Many studies have shown that the texture feature, as one of the three image features (morphology, color, and texture), can well reflect the overall characteristics of objects in the image from a macro scale. It is widely used for image recognition and image classification in various fields, such as medical science (Dhruv *et al.* 2019), remote sensing (Duan & Zhang 2021), and textiles (Wang *et al.* 2020), and it has a good application outlook due to its good stability, simple calculation, and the characteristic of non-individual analysis. Some studies have found that there is a good relationship between the texture features and the coagulation effect, which can be applied in predicting the coagulant dosage of wastewater treatment plants (Sivchenko *et al.* 2016), and based on this finding, a sensor was developed to optimize the control of coagulant dosage (Sivchenko *et al.* 2018). However, the study and application of texture analysis technology to water treatment is just getting started. The relationship between texture features and floc status, such as growth rate and settling velocity, remains to be explored.

In this study, the innovative application of the image texture feature to reflect the floc status will be deeply analyzed. Firstly, several jar tests were carried out under the same conditions, and the data stability was evaluated by comparing the morphological features with texture features. Secondly, the floc status and the corresponding texture features in different conditions were calculated and analyzed, trying to establish the relationship between them. In addition, the texture feature in various abnormal coagulation conditions was analyzed, and a detection method for abnormal conditions was summarized while verifying the results of this study. Our work provides a new perspective and technical approach for water quality improvement and process control in water plants.

2. MATERIALS AND METHODS

2.1. Raw water

The commercial kaolin (Kermel, Tianjin, China) was soaked in water for 24 h, and then the soaked kaolin and deionized water were used to prepare the raw water for the jar test (Wang *et al.* 2007). The turbidity was adjusted to 10 NTUs by changing the concentration of kaolin. The pH of raw water was measured using a multi-parameter water quality analyzer (DZS-708L, Leici, Shanghai, China) and maintained at 7.0 ± 0.05 with 1.0 mmol/L HCl and NaOH solution. The temperature of raw water was adjusted to room temperature (20 ± 0.5 °C).

2.2. Experimental design

Before and after coagulation, water samples were taken from 1 cm underneath the water surface, and the turbidity was measured by a turbidimeter (WGZ-20S, Xinrui, Shanghai, China). After a slow-mixing stage, 10 mL of water sample containing flocs was immediately sampled for settling velocity measurement. At the same time, another 10 μL water sample was taken for photomicrography. The sample was transferred with a pipette, in which the tip part was cut to gain a larger diameter opening to avoid the crushing of the floc (Mesquita *et al.* 2011). During the whole jar tests, the camera continuously captured *in situ* images of the flocs in the container.

2.3. Jar test

A 10 × 10 × 15 cm transparent cube container made of acrylic board was used for jar tests, and the volume of the water sample taken in each jar test was 1 L. Polymeric aluminum chloride (PAC) (Damao, Tianjin, China) with 30% alumina was used as a coagulant, and the dosage was expressed as PAC concentration. Mechanic mixing was done with an electric stirrer (GTCS-2014, Xinrui, Changzhou, China).

Several jar tests were done in the PAC dosage of 5–50 mg/L. Firstly the stirrer worked for 1 min at 200 rpm and then slowed down to 20 rpm and kept running for 15 min. At the end of mechanical mixing, the sample from 1 cm underneath the water surface was taken for turbidity measurement. According to the coagulant dosage with the lowest turbidity (Supplementary material, Table S1), the optimal coagulant dosage was 32 mg/L. Then, the orthogonal experiments were carried out to examine the four influencing factors (Quan *et al.* 2020). According to the result of orthogonal experiments (Supplementary material, Table S2), the optimal hydraulic conditions were determined as follows: 1 min fast-mixing at 200 rpm followed by 9 min slowing-mixing at 40 rpm. The testified optimal conditions were defined as the normal conditions for the jar tests in this study.

2.4. Settling velocity measurement

The settling velocity of flocs was measured by a self-made device as shown in Figure 1. The size of the settling column is 30 mm × 30 mm × 200 mm, and after the mixing phase, a 10 mL water sample was slowly injected into the settling column with distilled water from above. When the flocs had settled about 50 mm, the peristaltic pump was turned on, and

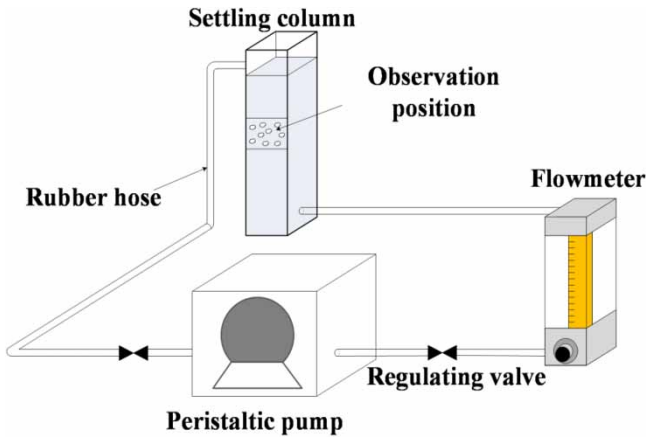

Figure 1 | Schematic diagram of the settling velocity measuring device.

the regulating valve was gradually opened, so that the settling velocity of flocs gradually decreased under the influence of the tiny reverse flow until the flocs were suspended at the observation port in the middle of the settling column. At this time, the rate of water flow indicated by the flowmeter was recorded, and then the settling velocity of the flocs could be determined according to the following formula:

$$v = \frac{Q \times 1,000}{A \times 60} \tag{1}$$

where v is the settling velocity (mm/s), Q is the rate of water flow (mL/min), and A is the cross-section area of the settling column (mm^2).

2.5. Image acquisition

The *in situ* image acquisition method of flocs is shown in Figure 2. The digital camera (D3500, Nikon, Japan) was set on the tripod and fixed at a proper height to ensure all flocs were in the frame. The settings of the image capture were specified as follows: exposure time 1/20 s, international standardization organization photo sensibility ISO-640, and taking an image every 10 s. The light source was 15 cm long and 3 cm wide LED light, the color temperature reached 5,600 K, and the brightness reached 552 lm. To ensure the handleability of images, a black card was placed behind the container as the background to make the flocs more visible in the image.

The microscopic image of flocs was acquired as follows: 10 μL of the water sample was placed on a slide and covered with a 20 mm × 20 mm coverslip, then the microscope (BX51, Olympus, Japan) and camera (DP72, Olympus, Japan) were used for image acquisition. With 40× magnification, 20 images were acquired from the area where flocs were not adhesion, three glass slides were used for each sample (Mesquita *et al.* 2011) to obtain a total of $3 \times 20 = 60$ images, which were stored in 1,920 × 1,080 pixels and a RGB format by the image acquisition software (Olympus, Japan).

2.6. Image processing and analysis

All images were processed using the image processing and analysis software ImageJ v2.3.0 (https://imagej.nih.gov/ij/) with the macro language. The processing of the *in situ* images is shown in Figure 3(a). A 350 × 450 pixels fixed area was selected for analysis. Such selection was made to avoid interference from the mixing paddle and the edge of the container. The *in situ* morphological features of the flocs, including area and particle size (expressed by the Feret diameter), were obtained with the

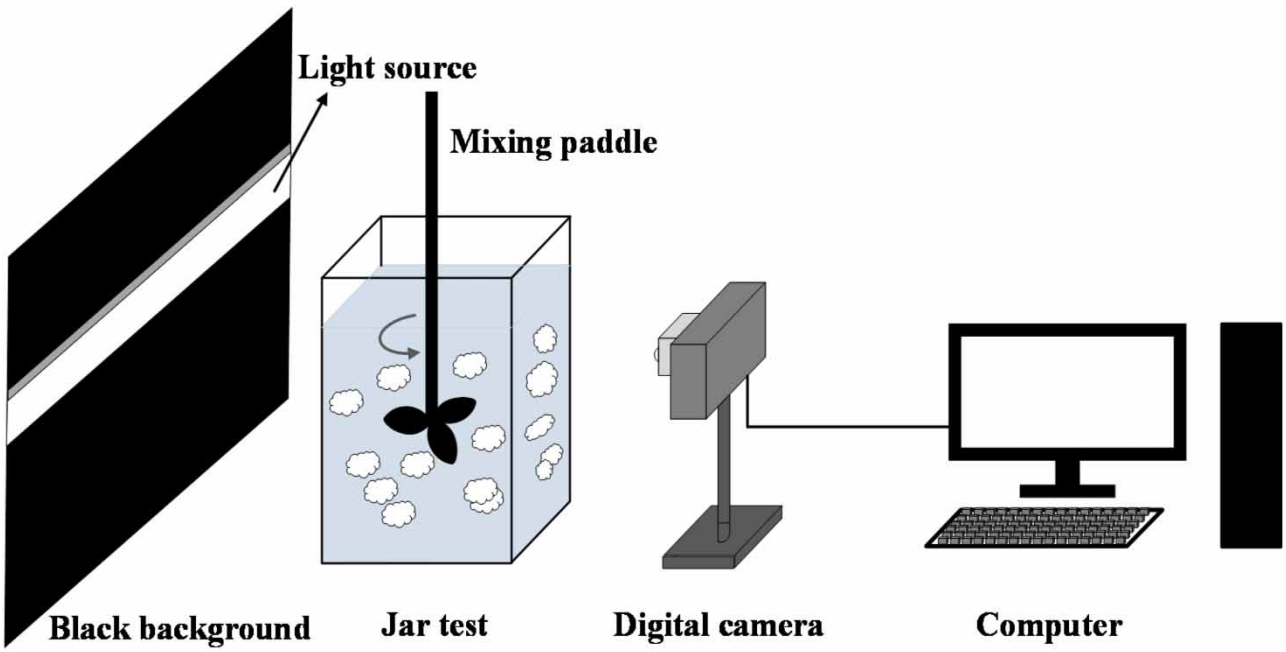

Figure 2 | Schematic diagram of *in situ* image acquisition.

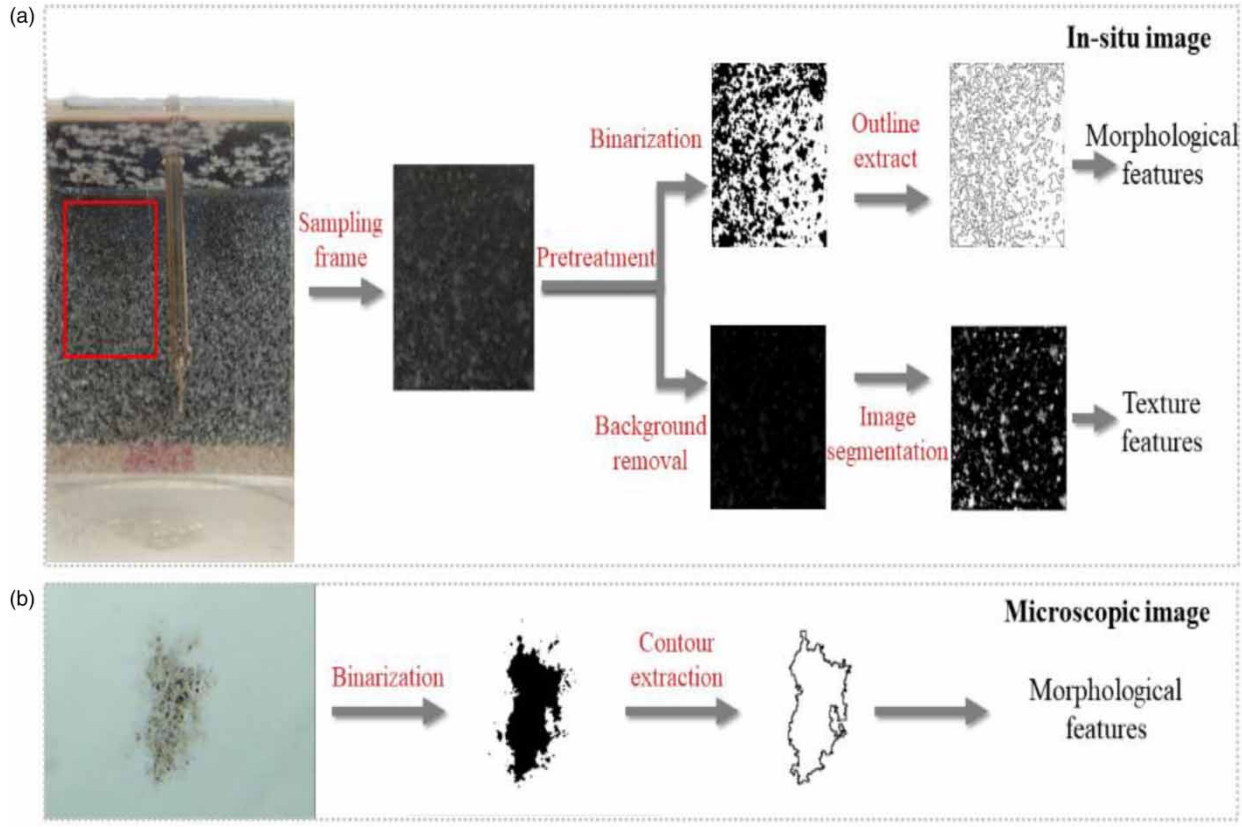

Figure 3 | The processing steps of floc images. (a) *In situ image* and (b) microscopic image.

'Analyze Particles' function. The fractal dimension was calculated by the method in a related study (Li *et al.* 2020). The texture features of the images were obtained by the gray level co-occurrence matrix (GLCM), which is a typical texture statistical measurement method (Haralick *et al.* 1973). Five texture features, including entropy, inverse difference moment, correlation, angular second moment, and contrast, were calculated by the plugin 'GLCM Texture' v.0.4 in ImageJ. Detailed explanations and formulas for GLCM can be found in other studies (Haralick *et al.* 1973; Widiyanto *et al.* 2018).

Microscopic morphological features were obtained from microscopic images, and the processing procedures are shown in Figure 3(b). The 'Analyze Particles' of ImageJ was used to get the area and particle size of flocs, and the calculation method of fractal dimension was the same as above.

2.7. Index to evaluate stability

Six jar tests in the normal condition were carried out. The parameters describing the microscopic morphological features, *in situ* morphological features, and texture features were obtained with the *in situ* images and microscopic images, which were acquired at the end of the slow-mixing stage (10 min). To compare the data stability, the coefficient of variation C_v was used to evaluate the fluctuation of various features. C_v was defined as follows:

$$C_v = \frac{\sigma}{\mu} \times 100\% \tag{2}$$

where σ is the standard deviation of data, and μ is the mean value of data.

2.8. Slope calculation of the texture time sequence curve curves

The texture feature values of the floc images, which were taken during the coagulation process, were arranged in a time order. The resulting data curve was called a texture time sequence curve (TTSC). Although the TTSC in each phase had small fluctuations and was not strictly straight, it was possible to be linearly fitted, and the slope of the fitted line was used for

quantitative evaluation. A similar method has been used to analyze the growth rate of flocs using the ratio curve of PDA (Ching *et al.* 1994; Wei *et al.* 2009). The linear fitting was achieved by the least square method, which was also used for other linear fitting mentioned in this study.

3. RESULTS AND DISCUSSION

3.1. Stability of texture features

In general, when an image feature is used to reflect the floc status, unstable data indicate that the feature is unsuitable for the current situation and has low credibility. Especially when applied to online monitoring, it is easy to cause wrong judgment, resulting in heavy losses.

Microscopic morphology and *in situ* morphology are common image features to reflect floc status in computational vision. As shown in Table 1, the C_v was high in both microscopic and *in situ* morphological features, especially for microscopic morphological features; the C_v of the floc area, particle size, and fractal dimension are as high as 44.0, 23.9, and 6.1%, respectively. However, the C_v of texture feature parameters represented by entropy and correlation (2.9 and 3.2%) was much lower than the C_v of microscopic morphological feature parameters and *in situ* morphological feature parameters. The instability of microscopic morphological features was due to the high sampling randomness of the flocs used for observation. It is difficult for the morphological feature of individual floc to reflect the whole, and this error was particularly significant when the number of samples was small. The instability of *in situ* morphological features was due to the serious adhesion and overlap between flocs when there are many flocs in the water, leading to the wrong information.

Compared with the morphological features of flocs, the texture features can represent the floc status more stably. In contrast to morphological features, texture features are not derived from the analysis of a single floc individually but are derived from a comprehensive analysis of the distribution, quantity, and shape of all flocs by analyzing the gray value of the image pixels (Shen *et al.* 2017), resulting in great integrity and high stability.

3.2. Selection of texture feature

The jar test was carried out under normal conditions, which was representative of *in situ* images of flocs obtained during coagulation and sedimentation as shown in Figure 4, and the TTSCs (including five texture feature parameters) are shown in Figure 5. By analyzing TTSCs, it can be found that the time sequential variations of the angular second moment, inverse difference moment, and correlation are very similar because they all reflect the distribution of gray values in the image but from different perspectives (Peddle & Franklin 1991). So, choosing one of them as the index to reflect the floc status shall be enough, and the inverse difference moment was selected due to its relative stability. In addition, the 'Enhance Contrast' operation was used for image processing, which can cause a large fluctuation of contrast. The contrast evaluates the difference of gray values between flocs and background in the image, and it can also be interpreted as the brightness of floc color (Haralick *et al.* 1973), which is not stressed in this study of the floc status. Therefore, the contrast was not chosen as the index. For entropy, it is an index to measure the complexity of image texture information. The more information and complexity of

Table 1 | Data stability comparison between the three representation methods of image features

	Microscopic morphological features			*In situ* morphological features			Texture features	
Sample	Area μm^2	Particle size μm	Fractal dimension –	Area μm^2	Particle size μm	Fractal dimension –	Entropy –	Correlation –
1	29,116	309.6	1.584	59,362	325.0	1.590	4.335	3.05×10^{-4}
2	43,339	383.3	1.842	55,306	316.7	1.580	4.251	3.24×10^{-4}
3	23,807	281.0	1.697	62,714	339.0	1.587	4.244	3.15×10^{-4}
4	34,514	339.6	1.618	61,359	328.0	1.617	4.391	2.97×10^{-4}
5	53,796	414.8	1.618	71,969	334.3	1.560	4.551	3.00×10^{-4}
6	12,810	199.6	1.575	32,826	264.3	1.761	4.211	3.10×10^{-4}
C_v (%)	44.0	23.9	6.1	23.0	8.6	4.5	2.9	3.2

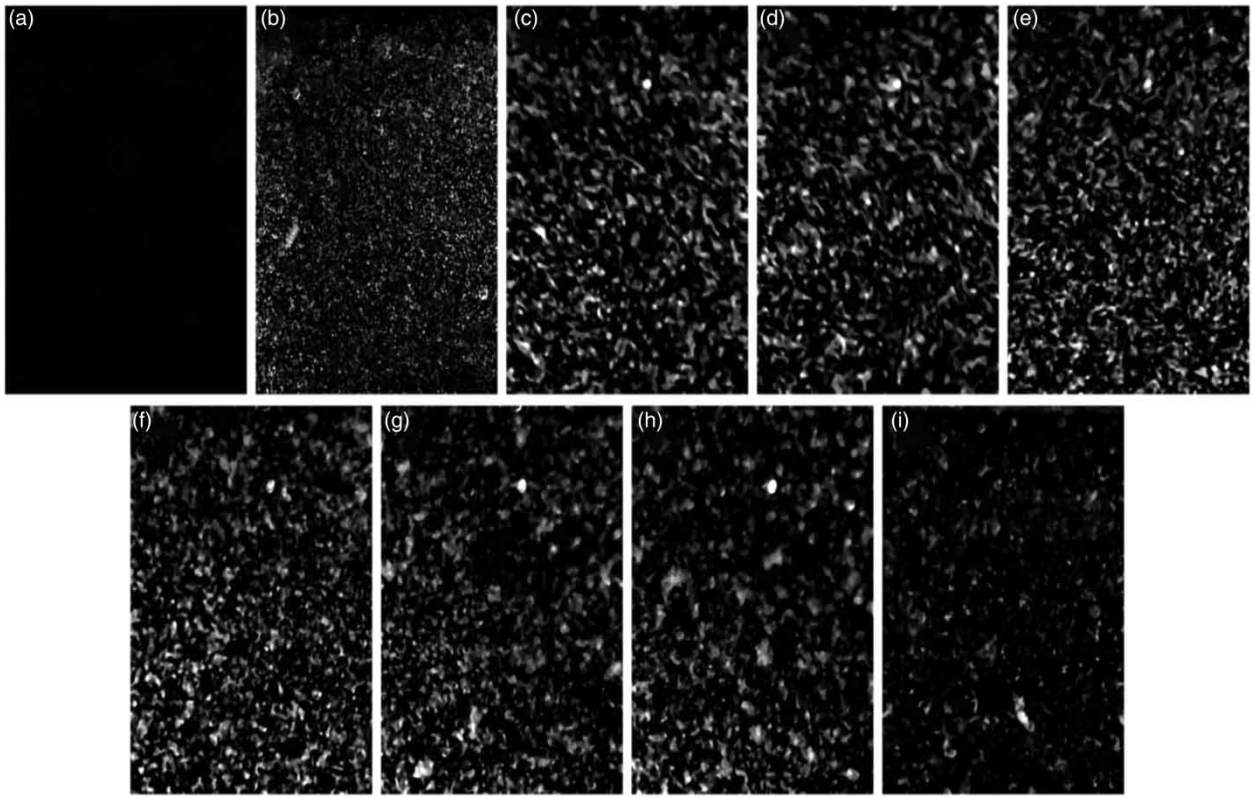

Figure 4 | Images of flocs acquired during coagulation and sedimentation. (a) 0 min, (b) 3 min, (c) 6 min, (d) 9 min, (e) 10 min, (f) 15 min, (g) 20 min, (h) 25 min, and (i) 30 min.

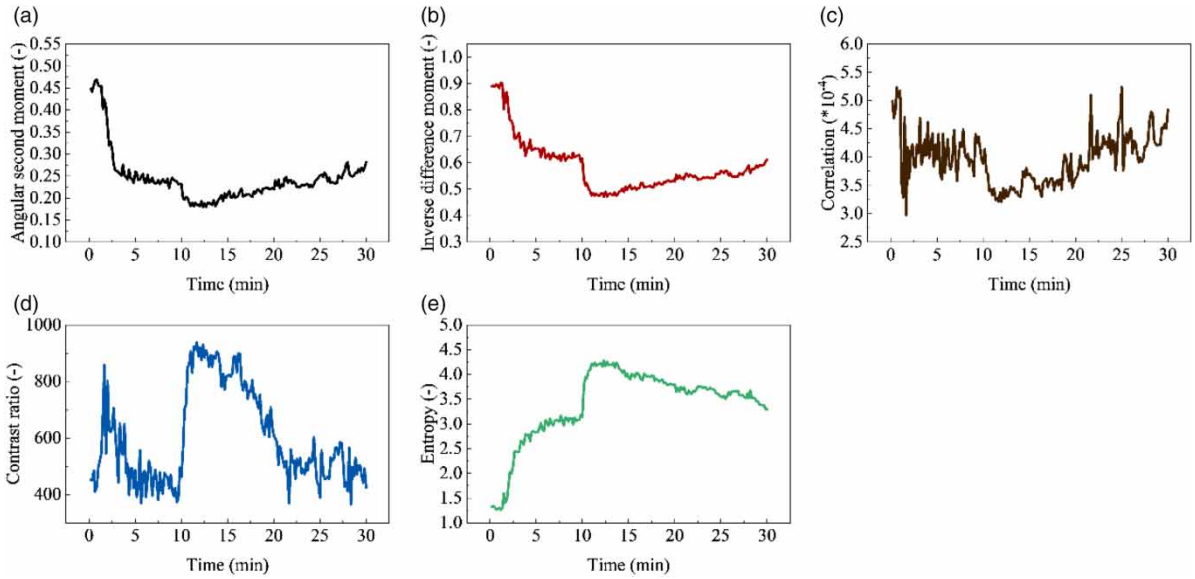

Figure 5 | Time sequence variation of different texture feature parameters in the normal condition. (a) Angular second moment, (b) inverse difference moment, (c) correlation, (d) contrast, and (e) entropy.

an image contains the higher the entropy. Including Figure 5, the data of many groups of experiments showed that the trend of inverse difference moment is in an opposite relationship with the entropy. Therefore, considering the simplification of the online monitoring setup, only one of the two parameters was needed to describe the flocculation.

The coagulation and sedimentation process includes the floc growth phase and the settling phase. As shown in Figure 4, in the growth phase, the flocs started to appear and grow from small to large, so the texture information of the images increased gradually, and the entropy increased accordingly. In the settling phase, many suspended flocs gradually settled to the bottom, resulting in a decrement of visible flocs in the image analysis area. Hence, the image texture information tapered, and the entropy also decreased accordingly. In conclusion, the entropy can be selected to monitor the floc status, including growth rate and settling velocity.

3.3. Representation of the growth rate by TTSC

According to the analysis in Section 3.2, the entropy can represent the floc growth rate in the coagulation process theoretically. To verify this assumption, the particle size and entropy of flocs in the growth phase were calculated by *in situ* images and plotted in the manner of time sequence. As an example, two sets of data obtained under different coagulation conditions are shown in Figure 6 (see Figure S1 for more examples). It can be found that the variation trends with the time of floc particle size and entropy show a strong consistency, which means that the change of entropy can be used to represent the change of particle size. Moreover, the growth rate is generally expressed by the ratio of particle size variation to time variation; in other words, by the slope of the particle size curve. Therefore, the slope of the TTSC can also be used to represent the growth rate of flocs.

In Figure 6(a), the TTSC in the growth phase of jar test 1 (normal condition) can be divided into three sections according to the slope. The flocs did not present in 0–80 s; within 80–260 s, the particle size increased to 527 μm but only grew 53 μm in the following 260–600 s. It showed that floc growth has three stages with different growth rates, namely micro-flocculation stage, fast growth stage, and stable stage, the same as previous studies reported (Wei *et al.* 2009). However, different from Figure 6(a), the TTSC in Figure 6(b) entered the fast growth stage with a low slope when it approached 200 s. Jar test 2 was in abnormal conditions, as the fast-mixing time set in this group was only 10 s and far lower than 60 s in normal conditions. Consequentially, the coagulant hydrolyzed and dispersed slowly in water, resulting in delayed formation and slow growth of flocs. These results showed that the TTSC can not only represent the growth rate of flocs but also indicate the abnormal conditions of the coagulation process.

3.4. Representation of the settling velocity by the TTSC

As shown in Figure 4, during the settling phase, the number of flocs in the image gradually decreased with the floc settling. Therefore, the gray value of most pixels went down to 0, resulting in the reduction of image texture information, so the entropy also decreased gradually. It can be concluded that the faster the settling velocity of flocs, the faster the entropy decreases, which leads to a steeper TTSC.

In order to verify the feasibility of using the TTSC slope to represent the settling velocity of flocs in the settling phase, 72 groups of the jar test were carried out under different conditions. The relationship between the TTSC slope and the settling velocity of each group is shown in Figure 7. It can be found that there is a pronounced linear correlation between them, the fitting relation was $y = -9.8056x + 0.1430$, $R^2 = 0.5318$, and the fitting was good even with all 72 groups of data. This result

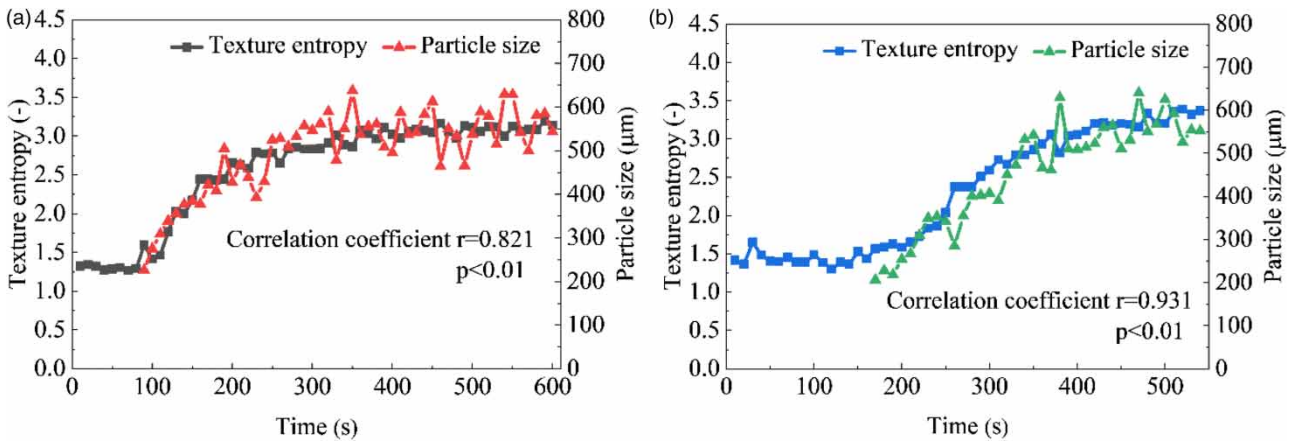

Figure 6 | Sequential variation of floc particle size and texture entropy in the growth phase under normal condition. (a) Jar test 1 and (b) jar test 2.

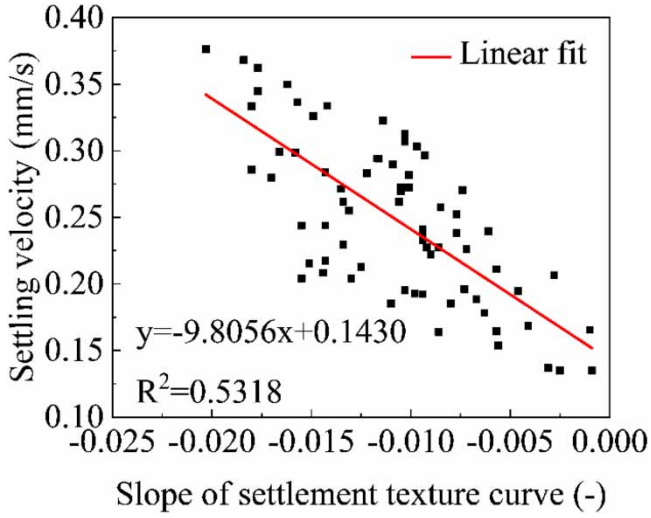

Figure 7 | The relationship between the settling velocity and the TTSC slope in the settling phase.

suggested that the TTSC slope in the settling phase can well represent the settling velocity of flocs; the higher the slope, the higher the settling velocity.

Furthermore, among the 72 groups of experiments, the conditions of many groups were seriously different from the normal condition. For example, the dosage of coagulant in some groups was only 5 mg/L, which was insufficient for proper flocculation, so these groups could be considered as abnormal condition groups. However, the results have proved that the TTSC slope also correlated well with the settling velocity of flocs under abnormal conditions. Therefore, the TTSC can identify abnormal conditions of flocculation by indicating settling velocity.

3.5. Identification of abnormal conditions

In order to simulate the coagulation process in different abnormal conditions, based on the normal condition, six factors, including mixing speed, mixing time, turbidity, coagulant dosage, temperature, and pH, which can greatly influence the coagulation effect, were changed to carry out the jar test. The TTSC in abnormal conditions was compared with it in the normal condition, and the abnormal features of the curve were analyzed.

The abnormal condition of the fast-mixing speed is shown in Figure 8(a). The TTSC in the normal condition (200 rpm) entered the fast growth stage was around 1.5 min, while the abnormal condition (50 rpm) was around 3.5 min. When the fast-mixing speed was not enough, the coagulant could not disperse evenly and hydrolyze quickly in the water, so the flocs were generated slowly in the early stage. It took longer for the flocs to grow to a specific size and enter the fast-growth stage.

The abnormal condition of the slow-mixing speed is shown in Figure 8(b). Compared with the normal condition (40 rpm), the slope of the TTSC in the abnormal condition (80 rpm) was lower in the fast growth stage. When it was around 4 min, the slope began to drop to 0, flocs entered the stable stage, and the slope was also lower in the settling stage. Due to the disturbance of water flow, it was difficult for the tiny floc to have an effective collision when the slow-mixing speed was too high, resulting in a slow growth rate. The generated flocs were also easily stirred and broken by the strong water flow, and it was difficult to form larger flocs, so they entered the stable stage early and settled slowly in the settling stage.

The abnormal condition of the fast-mixing time is shown in Figure 8(c). Compared with the normal condition (1 min), the TTSC in the abnormal condition (10 s) entered the fast growth stage later (at about 2.5 min), but their slope in the fast growth stage and the settling stage was almost the same. When the fast-mixing time was insufficient, the coagulant could not be thoroughly dispersed in water, resulting in the slow formation of flocs, so they entered the fast growth stage late. However, due to the sufficient slow-mixing time, the flocs with good settling velocity can eventually form.

The abnormal condition of the slow-mixing time is shown in Figure 8(d). Compared with the normal condition (9 min), the slope of the TTSC in the abnormal condition (1 min) was close to 0 in the settling stage. When the slow-mixing time was insufficient, only extremely tiny flocs that were barely visible could be formed, so they were suspended in water without settling in the settling stage.

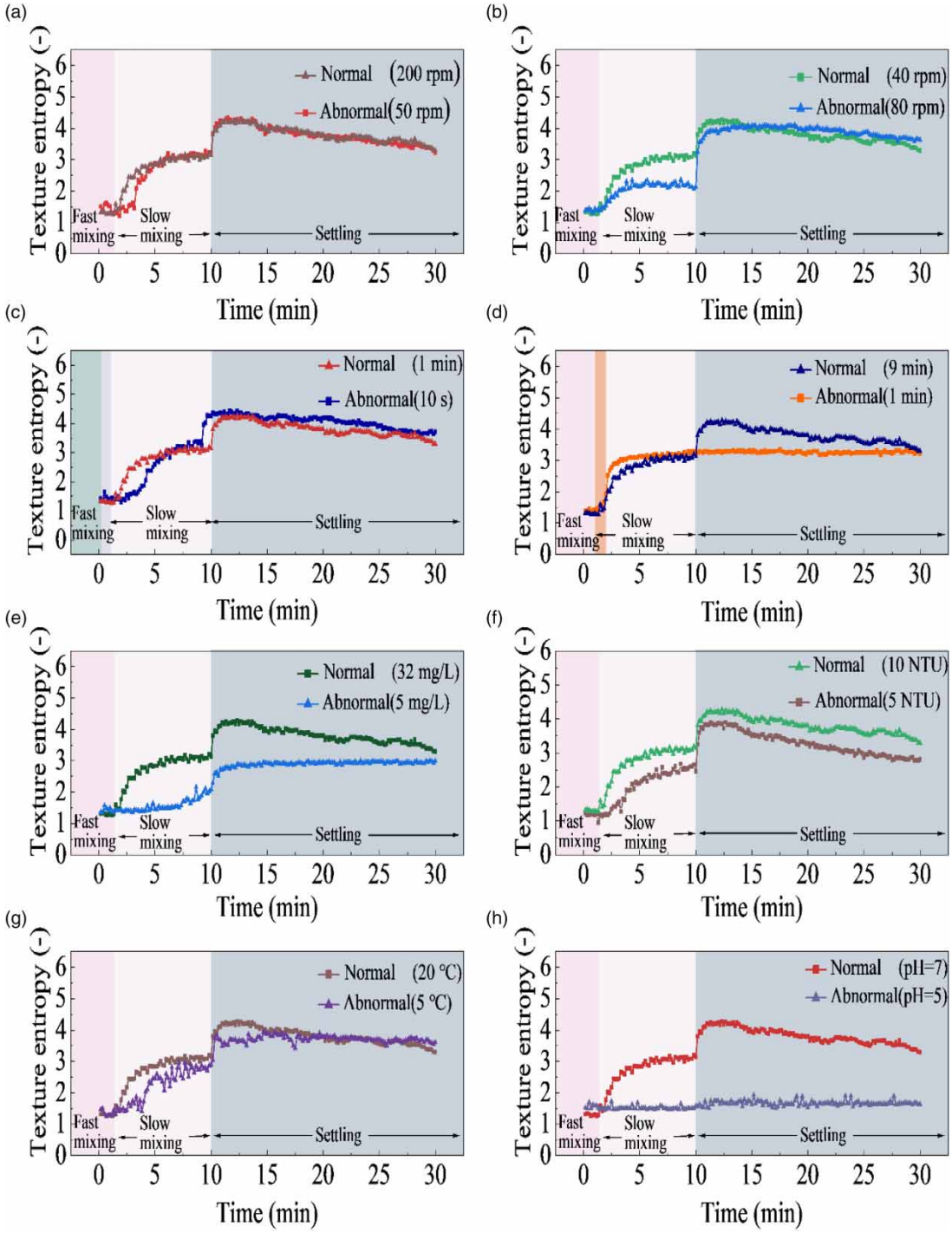

Figure 8 | Comparison of TTSCs in normal and different abnormal conditions. (a) Fast-mixing speed, (b) slow-mixing speed, (c) fast-mixing time, (d) slow-mixing time, (e) dosage of coagulant, (f) turbidity, (g) temperature, and (h) pH.

The abnormal condition of the coagulant dosage is shown in Figure 8(e). Compared with the normal condition (32 mg/L), the TTSC in the abnormal condition (5 mg/L) just entered the fast growth stage at about 8.5 min with a low slope, and the slope of the TTSC in the settling stage was close to 0. When the coagulant dosage was insufficient, the flocs aggregated slowly, requiring a longer mixing time to aggregate into tiny flocs, and such tiny flocs could hardly settle.

The abnormal condition of the turbidity is shown in Figure 8(f). Compared with the normal condition (10 NTUs), the TTSC in the abnormal condition (5 NTUs) had a lower slope and a longer duration in the fast growth stage, but there is no significant difference in their slope in the subsequent settling stage. When the turbidity was low, the possibility of collisions between particles was small, and it was difficult to have effective collisions, so the flocs grew slowly. However, flocs with good settling ability can be generated eventually through sufficient mixing time.

The abnormal condition of the temperature is shown in Figure 8(g). Compared with the normal condition (20 °C), the slope of the TTSC in the abnormal condition (5 °C) was lower in the fast growth stage and close to 0 in the settling stage. The hydrolysis process of coagulant is an endothermic reaction when the temperature is low, and slow hydrolysis affects the destabilization of the colloidal particles. Meanwhile, the low temperature will also increase water viscosity and hinder flocs' aggregation, so the tiny flocs formed are difficult to settle.

The abnormal condition of the pH value is shown in Figure 8(h). Compared with the normal condition (pH = 7), the TTSC in the abnormal condition (pH = 5) did not rise in the whole process of coagulation, and the slope was always 0. When the pH of water is too low, the high positive charge of PAC will rapidly change the surface potential of the particles, making the colloidal particles quickly change from a stable state with a negative charge to a stable state with a higher positive charge. In addition, H^+ will also limit the effective flocculation of the polynucleated hydroxyl polymer when the pH is low, so the particles in the water were difficult to aggregate into flocs while keeping stable.

The above results showed that the TTSC in many kinds of abnormal conditions has its unique abnormal features, which indicated that the abnormal conditions of coagulation can be well identified by analyzing the TTSC. Moreover, the characteristics of the coagulation process in various abnormal conditions were well explained and verified by the TTSC. It again proved the feasibility and credibility of using this method to reflect the floc status.

3.6. Practical implications

Based on the texture feature of floc images, this method may be further developed as an actual sensor for online monitoring and abnormal condition identification. In the practice field, cameras and light sources can be sealed in waterproof stainless-steel cases and put into coagulation tanks and sedimentation tanks. The real-time floc images will be transmitted to the computer for analysis. The analysis system should include the automatic GLCM texture extraction algorithm and the TTSC analysis algorithm developed based on the findings of this study. Furthermore, if combined with smartphone and internet technology, it will be helpful to the safety of drinking water in remote and underdeveloped regions.

4. CONCLUSIONS

In this paper, the application of image texture features in monitoring floc growth and the settling process was investigated. We found that the TTSC of floc images could well reflect the flocculation process. The slope of the TTSC during the growth phase and the TTSC during the settling phase can describe the growth rate and the settling velocity, respectively, i.e., the higher the slope, the higher the growth rate and the settling velocity. In addition, the TTSC in different abnormal conditions all showed their own abnormal features, so the change characteristics of TTSC can be used to identify many kinds of abnormal conditions well.

In summary, the findings in this study provided a novel approach to evaluate the floc status and recognize abnormal conditions during the coagulation and sedimentation process by using the TTSC. This approach is easy to use and reliable and can represent the growth rate and the settling velocity of flocs by just one curve, which is difficult to achieve by other methods. The proposed method could be developed into a simple and economical tool for the management of WTP, especially for online monitoring of the flocs, and may inspire further studies in the future.

ACKNOWLEDGEMENTS

This work was supported by the National Natural Science Foundation of China (52070149 and 51878539).

DATA AVAILABILITY STATEMENT

All relevant data are included in the paper or its Supplementary Information.

CONFLICT OF INTEREST

The authors declare there is no conflict.

REFERENCES

Adachi, Y. & Tanaka, Y. 1997 Settling velocity of an aluminium-kaolinite floc. *Water Research* **31** (3), 449–454.

Bo, X., Gao, B., Peng, N., Wang, Y., Yue, Q. & Zhao, Y. 2012 Effect of dosing sequence and solution pH on floc properties of the compound bioflocculant-aluminum sulfate dual-coagulant in kaolin-humic acid solution treatment. *Bioresource Technology* **113**, 89–96.

Ching, H.-W., Tanaka, T. S. & Elimelech, M. 1994 Dynamics of coagulation of kaolin particles with ferric chloride. *Water Research* **28** (3), 559–569.

Dhruv, B., Mittal, N. & Modi, M. 2019 Study of Haralick's and GLCM texture analysis on 3D medical images. *International Journal of Neuroscience* **129** (4), 350–362.

Duan, M. & Zhang, X. 2021 Using remote sensing to identify soil types based on multiscale image texture features. *Computers and Electronics in Agriculture* **187**, 106272.

Ekeleme, A. C., Ekwueme, B. N. & Agunwamba, J. C. 2021 Modeling contaminant transport of nitrate in soil column. *Emerging Science Journal* **5** (4), 471–485.

Haralick, R. M., Shanmugam, K. & Dinstein, I. H. 1973 Textural features for image classification. *IEEE Transactions on Systems, man, and Cybernetics* **3** (6), 610–621.

Ismail, W. N. W., Syah, M. I. A. I., Abd Muhet, N. H., Bakar, N. H. A., Yusop, H. M. & Samah, N. A. 2022 Adsorption behavior of heavy metal ions by hybrid inulin-TEOS for water treatment. *Civil Engineering Journal* **8** (9), 1787–1798.

Li, Z.-H., Han, D., Yang, C.-J., Zhang, T.-Y. & Tu, H.-Q. 2019 Probing operational conditions of mixing and oxygen deficiency using HSV color space. *Journal of Environmental Management* **232**, 985–992.

Li, Z.-H., Guo, Y., Hang, Z.-Y., Zhang, T.-Y. & Yu, H.-Q. 2020 Simultaneous evaluation of bioactivity and settleability of activated sludge using fractal dimension as an intermediate variable. *Water Research* **178**, 115834.

Liu, Y., Zhang, X., Jiang, W., Wu, M. & Li, Z. 2021 Comprehensive review of floc growth and structure using electrocoagulation: characterization, measurement, and influencing factors. *Chemical Engineering Journal* **417**, 129310.

Matilainen, A., Vepsalainen, M. & Sillanpaa, M. 2010 Natural organic matter removal by coagulation during drinking water treatment: a review. *Advances in Colloid and Interface Science* **159** (2), 189–197.

Mesquita, D., Amaral, A. & Ferreira, E. 2011 Identifying different types of bulking in an activated sludge system through quantitative image analysis. *Chemosphere* **85** (4), 643–652.

Moruzzi, R. B., Da Silva, P. G., Sharifi, S., Campos, L. C. & Gregory, J. 2019 Strength assessment of Al-humic and Al-kaolin aggregates by intrusive and non-intrusive methods. *Separation and Purification Technology* **217**, 265–273.

Peddle, D. R. & Franklin, S. E. 1991 Lmage texture processing and data integration. *Photogrammetric Engineering and Remote Sensing* **57**, 413–420.

Peña-Guzmán, C. & Ortiz-Gutierrez, B. E. 2022 Evaluation of three natural coagulant from *Moringa oleifera* seed for the treatment of synthetic greywater. *Civil Engineering Journal* **8** (12), 3842–3853.

Quan, H., Guo, Y., Li, R., Su, Q. & Chai, Y. 2020 Optimization design and experimental study of vortex pump based on orthogonal test. *Science Progress* **103** (1), 0036850419881883.

Shen, X., Shi, Z. & Chen, H. 2017 Splicing image forgery detection using textural features based on the grey level co-occurrence matrices. *IET Image Processing* **11** (1), 44–53.

Sivchenko, N., Kvaal, K. & Ratnaweera, H. 2016 Evaluation of image texture recognition techniques in application to wastewater coagulation. *Cogent Engineering* **3** (1), 1206679.

Sivchenko, N., Kvaal, K. & Ratnaweera, H. 2018 Floc sensor prototype tested in the municipal wastewater treatment plant. *Cogent Engineering* **5** (1), 1436929.

Tomperi, J., Koivuranta, E., Kuokkanen, A., Juuso, E. & Leiviskä, K. 2016 Real-time optical monitoring of the wastewater treatment process. *Environmental Technology* **37** (3), 344–351.

Vahedi, A. & Gorczyca, B. 2012 Predicting the settling velocity of flocs formed in water treatment using multiple fractal dimensions. *Water Research* **46** (13), 4188–4194.

Wang, G., Wang, X. & Jin, P. 2007 Coagulation condition of kaolin suspended particles and their morphological characteristics with PAC dosage. *Water & Wastewater Engineering* **33** (11), 143–145.

Wang, W., Deng, N., Xin, B., Wang, Y. & Lu, S. 2020 Novel segmentation algorithm for jacquard patterns based on multi-view image fusion. *IET Image Processing* **14** (17), 4563–4570.

Wei, J., Gao, B., Yue, Q. & Wang, Y. 2009 Effect of dosing method on color removal performance and flocculation dynamics of polyferric-organic polymer dual-coagulant in synthetic dyeing solution. *Chemical Engineering Journal* **151** (1–3), 176–182.

Widiyanto, S., Sukra, Y., Madenda, S., Wardani, D. T. & Wibowo, E. P. 2018 Texture feature extraction based on GLCM and DWT for beef tenderness classification. In *2018 Third International Conference on Informatics and Computing (ICIC)*. IEEE, pp. 1–4.

Wu, C., Wang, Y., Gao, B., Zhao, Y. & Yue, Q. 2012 Coagulation performance and floc characteristics of aluminum sulfate using sodium alginate as coagulant aid for synthetic dying wastewater treatment. *Separation and Purification Technology* **95**, 180–187.

Xiao, F., Lam, K. M., Li, X., Zhong, R. & Zhang, X. 2011 PIV characterisation of flocculation dynamics and floc structure in water treatment. *Colloids and Surfaces A: Physicochemical and Engineering Aspects* **379** (1–3), 27–35.

First received 18 January 2023; accepted in revised form 28 August 2023. Available online 11 September 2023